

Chapter 6

Photolysis of Pyruvic Acid in Ice. Possible Relevance to CO and CO₂ Ice Core Record Anomalies

Submitted for publication in the *Journal of Geophysical Research*, M. I. Guzmán, A. J. Colussi, and M. R. Hoffmann, August, 2006

Abstract

The abnormal spikes detected in ice core CO and CO₂ records reveal chemical activity in deep sections by processes that forgo diffusional approach. The correlation of CO and CO₂ excesses with CO/CO₂ yields in the photolysis of natural organic matter would support a photochemical process if such matter were coextensive with the spikes and a source of actinic radiation could be identified. We showed that the UV radiation generated by cosmic muons could account for the irregularities found in some CO records, should the photolysis of natural organic matter proceed with similar yields in water and ice. We find that the photodecarboxylation of pyruvic acid (PA, an ice contaminant) actually occurs by the same mechanism, and nearly as efficiently, in both media. CO₂ is promptly released by frozen PA/H₂O films upon illumination, but continues to evolve after photolysis. The concerted photodecarboxylation of benzoylformic acid (the aryl analogue of PA) does not yield post-illumination CO₂ under similar conditions. We infer that ³PA* reacts with PA to produce acetylcarbonyloxyl, CH₃C(O)C(O)O·, and ketyl, CH₃Ċ(OH)C(O)OH, as primary intermediates. The barrierless decarboxylation: CH₃C(O)C(O)O· → CH₃C(O)· + CO₂, accounts for CO₂(g) emissions under cryogenic conditions. Bimolecular radical reactions ensue leading to species that undergo protracted decarboxylation. The latter involves metastable species whose decay is controlled by morphological relaxations of the ice matrix. The quantum yield of CO₂ production in the photolysis of PA at λ ~ 313 nm drops from φ_{CO₂} = 0.78 in water at 293 K to φ_{CO₂} = 0.29 in ice at 250 K.

Introduction

Gas bubbles trapped in deep ice could be intact remnants of Earth's paleoatmospheres.¹⁻⁶ If so, the correlation between CO₂ concentrations in ancient ice bubbles and global ambient temperatures at the time of trapping (as reported by ¹⁸O or ²H abundances in the ice)^{2,7} would be a significant, although perhaps not definitive,⁸⁻¹⁰ precedent to the potential climatic effects of anthropogenic CO₂ emissions.

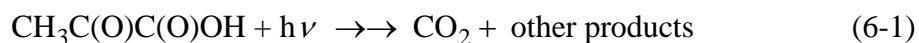
Air extracted from polar ice registers exponentially rising atmospheric CO₂ concentrations (from pre-industrial ~ 280 ppmv levels) during the last two centuries. However, higher CO₂ concentrations also accompanied the transition from the last glaciation period to the Holocene.¹¹ More ominously, some records appear to be tainted by *in situ* processes that remain to be characterized. Thus, Siple Dome CO₂ ice core records contain anomalous sections that are not replicated in other Antarctic sites.¹² Greenland records dating from the last two millenia display CO₂ concentrations that exceed (by up to ~ 20 ppmv) those in coeval Antarctic sites.^{13,14} The discrepancies: (1) are localized in thin sections representing less than two annual periods, i.e., intervals much shorter than the decades elapsing between snow deposition and gas encapsulation, (2) are larger than the precision of measurements (± 3 ppmv) and, (3) cannot be ascribed to interhemispheric gradients.¹⁵ The international scientific community seeks to understand the causes of such anomalies and, hence, identify secure Antarctic ice cores.

The irregular records reflect chemical activity under rather unusual conditions, because the production of excess carbon oxides involves precursors frozen in ice at hundreds of meters below the surface, i.e., immobilized at low temperatures in the complete absence of sunlight. Together, these findings undermine the fundamental

assumption that the chemical identity of matter embedded in glacial ice is indefinitely preserved. Several mechanisms have been proposed to account for this phenomenon. Carbon dioxide could originate from the acidification of carbonate deposits^{16,17} or the oxidation of organic matter.¹¹ However, some CO records are also exceedingly irregular,¹⁴ although CO is a reduced carbon species that cannot be produced by acidification of carbonate. The nearly constant ~ 50 ppbv CO levels detected in the Vostok (Antarctica) ice core are not replicated by Eurocore (Greenland) readings, which display greater variability, reaching up to 180 ppbv in layers antedating ~ 1500 AD.^{11,14,18} Concentration spikes seem to be otherwise incompatible with mechanisms involving the diffusional approach of putative precursors in polycrystalline ice.

The possibility of photochemistry in deep ice has been apparently dismissed due to the lack of conceivable sources of *in situ* actinic radiation. At variance with thermal bimolecular thermal reactions, photochemical transformations are (nearly) temperature-independent unimolecular events. The detection of ultraviolet radiation generated by penetrating muons of cosmic origin in deep Antarctic ice,¹⁹⁻²¹ and the finding that Greenland ice cores are contaminated with organic matter released by medieval forest fires in the Northern Hemisphere,^{22,23} are highly significant in this context. Humic-like substances,²⁴⁻³¹ such as those present in natural waters, atmospheric aerosol, and polar ice,^{22,32-37} are known to be photodegraded into carbon oxides by sunlight. Isolated chromophores associated with the sporadic contamination of glacial ice by humic-like matter could sustain significant photochemistry in the perennial photon field present deep in the polar caps.³⁸ Organic photochemistry in ice is, however, a largely unexplored subject. In order to provide factual support to the notion that *in situ* photochemistry of

natural organic matter may be the source of carbon oxides in deep ice, we report on the photodecarboxylation of the environmentally ubiquitous pyruvic acid (2-oxopropanoic, PA)²² in frozen aqueous solutions, reaction 6-1:³⁹⁻⁴²



Experimental Section

100 mM PA (Aldrich 98.0%, bidistilled at reduced pressure) or 10 mM benzoylformic acid (BF; Aldrich 97%, used as received) solutions in Milli-Q water were acidified to pH 1.0 with perchloric acid (Mallinckrodt, 70% analytical reagent) prior to photolysis. More than 98% of the CO₂ is released into the gas phase from thawed, photolyzed solutions, while the “other products” of reaction 6-1 remain in solution. Fluid or frozen solution samples (4 mL) were photolyzed in a reactor consisting of a cylindrical chamber fitted with an axial silica finger housing a UV lamp (Hg Pen-Ray model CPQ 8064, emitting at 313 ± 20 nm), and connected to the infrared cell (CaF₂ windows, 10 cm optical path) of a Bio-Rad Digilab FTS-45 FTIR spectrometer for the continuous monitoring of CO₂(g) via online absorption infrared spectrophotometry at 2349 cm⁻¹. The gases contained in the (reactor + IR cell) assembly were recirculated (by means of a Schwartzer model 135 FZ micropump) every ~ 4 s. Reactor temperature was controlled by immersion into a thermostat/cryostat (Neslab ULT-80) filled with methanol. Low-temperature experiments involved irradiation of 1 mm thick ice layers produced by freezing aqueous solutions (4 mL, previously sparged with N₂ or O₂ at 293 K for 30 min) onto the outer reactor chamber walls. Ice layers were maintained at the target temperatures for at least 2 hours prior to photolysis, which were carried with the reactor filled with 1 atm N₂ or O₂. We performed blank experiments maintaining the UV lamp on

to confirm there was no considerable temperature difference between a thermocouple located on the surface of the ice layer and the cooling bath where the reactor was immersed. Additionally, due to the fast recirculation of the gas, we discard heat transfer problems in the timescale of our variable temperature experiments. Sample absorption and lamp emission spectra were recorded with a HP 8452A diode array spectrophotometer. Quantum yield (ϕ_{CO_2}) measurements were based on the photolysis of BF, reaction 6-2



as chemical actinometer.⁴³ Aqueous solutions of the radical scavenger 2,2,6,6-tetramethylpiperidin-1-oxyl (TEMPO, Aldrich 99%, purified by vacuum sublimation) were used in some experiments.⁴² Control dark experiments confirmed that PA and BF are thermally stable under present reaction conditions: $227 \text{ K} < T < 278 \text{ K}$, 3 hours.

Organic product analysis were performed via HPLC at ambient temperature, using UV and electrospray ionization-mass spectrometric (ESI MS) detection (Agilent 1100 series Model 1100 Series HPLC-MSD System), immediately after sample melting.⁴²

Results and Discussion

CO₂(g) Photogeneration

Figure 6-1 shows the release of CO₂(g) during and after irradiation of frozen aqueous PA layers maintained at 248 K. Additional CO₂(g) is liberated upon melting the ice layers. Plotted CO₂(g) values correspond to moles of CO₂(g) normalized to the fluid volume of PA layers (4×10^{-3} L). CO₂(g) is immediately detected, and continues to evolve at nearly constant rates, upon irradiation at temperatures down to $\sim 130 \text{ K}$. This

lower limit corresponds to the temperature range in which the sublimation pressure of solid CO₂ falls below instrumental sensitivity.⁴¹ Post-irradiation CO₂(g) is emitted at rates that slow down as $\exp(-k_D \times \text{time})$ (Figure 6-2). Neither CO nor CH₄ were detected as gas-phase products in these experiments.

About 1.54 μmoles of CO₂ are released at the end of photolysis at 248 K. Additional CO₂ (up to a total of 1.87 μmoles of CO₂) is slowly released from irradiated frozen samples maintained at the same temperature (Figure 6-2). From the 400 PA μmoles contained in the frozen layers, about 1% are photochemically transformed into the 4.28 μmoles of CO₂ that are detected after melting irradiated samples (Figure 6-1). Thus, about half of the photogenerated CO₂ ultimately escapes from frozen layers via a porous network open to the atmosphere, while the rest remains indefinitely trapped in the solid. The CO₂(g) amounts released after each stage as a function of experimental temperature are shown in Figure 6-3. The apparent enthalpy change associated with overall CO₂(g) production, i.e., with the total CO₂(g) amounts recovered after melting, $\Delta H = (6.44 \pm 1.55) \text{ kJ mol}^{-1}$, is remarkably similar to the enthalpy of ice melting: $\Delta H_M = 6.30 \text{ kJ mol}^{-1}$.

The post-illumination emissions of CO₂(g) from irradiated frozen PA solutions is not due to the slow release of preformed CO₂ from the ice matrix, but arises from an ongoing dark chemical reaction. Otherwise, we would have observed the same phenomenon in irradiated frozen BF solutions, at variance with the results shown in Figure 6-4. The lack of post-illumination CO₂(g) emissions from frozen BF solutions rules out a purely physical explanation for the substantial amounts of CO₂(g) released from their PA counterparts. These contrasting behaviors arise from the fact that BF photodecarboxylation (reaction 6-2) occurs in one step,⁴³ while PA photolysis proceeds

via reactive intermediates.⁴² Therefore, unless further CO₂ is produced in the dark, the CO₂ photogenerated in ice cavities connected to the gas phase is released fully and promptly (i.e., within a few seconds). The stepwise warming of pre-irradiated frozen PA samples reveals that additional CO₂ is produced at each temperature jump, which is released with rate constants k_D that also increase with temperature. Rate constants k_D measured in isothermal experiments (Figure 6-5) follow the Arrhenius expression:

$$\log(k_D/s^{-1}) = 1.08 - 1191/T \quad (6-3)$$

which corresponds to an apparent activation energy: $E_{a,D} = 22.8 \text{ kJ mol}^{-1}$, and A-factor: $A_D = 12.1 \text{ s}^{-1}$ (see below).

The photolysis of PA in water, which is known to proceed via a free radical mechanism, is partially inhibited by radical scavengers⁴² such as the persistent nitroxide radical scavenger 2,2,6,6-tetramethylpiperidin-1-oxyl (TEMPO).⁴⁴⁻⁴⁶ Photochemical CO₂(g) production rates in fluid aqueous PA solutions drop by about 55% for [TEMPO] $\geq 1.7 \text{ mM}$.⁴² In contrast, TEMPO has no effect on CO₂(g) production rates during the photolysis of PA solutions frozen under 1 atm N₂ (Figure 6-6), or those measured in the post-illumination stage. The efficiency of TEMPO as a radical scavenging cosolute is seemingly forfeited in frozen media by mobility restrictions. O₂(g), in contrast, acts as a weak inhibitor both in fluid⁴³ and frozen solutions: CO₂(g) production rates in the photolysis of frozen PA solutions performed under 1 atm O₂ are ~ 25% slower than under 1 atm N₂ at 253 K.

Quantum yields for the overall production of CO₂(g) in reaction 6-1, ϕ_{CO_2} , in fluid and frozen aqueous PA solutions were determined from: (1) measured rates of CO₂(g) evolution above aqueous solutions under continuous illumination and, (2) the CO₂(g)

amounts recovered from frozen solutions that had been irradiated at constant temperature T for specified periods of time and subsequently thawed. The effective absorption coefficients, ϵ_{eff} 's, of PA and BF in these experiments were evaluated from the convolution of their experimental absorption spectra in aqueous solution with the emission spectrum of the lamp. Since the extent of the partial hydration of keto-PA (k -PA), the actual chromophoric species, into 2,2-dihydroxypropanoic acid (h -PA), is an inverse function of temperature, the ϵ_{eff} of PA determined in water at 293 K was scaled down [$\epsilon_{\text{eff}}(< 270\text{K}) = 0.69 \times \epsilon_{\text{eff}}(293 \text{ K})$] in frozen solutions by the k -PA concentrations calculated from the experimental ratios: $[h\text{-PA}]/[k\text{-PA}] = 2.54$ (293 K) and 4.10 ($T < 270$ K).⁴⁷⁻⁴⁹ BF is barely hydrated under present conditions.⁵⁰ We assumed that the quantum yield of CO_2 formation in the concerted photodecarboxylation of aqueous BF solutions ($\phi_{\text{CO}_2, \text{BF}} = 0.39$ at pH 3.0, 298 K)^{43,51} does not change with physical state or temperature (cf. with the intramolecular photoisomerization of 2-nitrobenzaldehyde).⁵² Photolysis experiments in fluid and frozen BF or PA solutions led to $\phi_{\text{CO}_2} = 0.78 \pm 0.10$ in water at 293 K (in excellent agreement with Leermakers and Vesley,⁵³ and to the expression

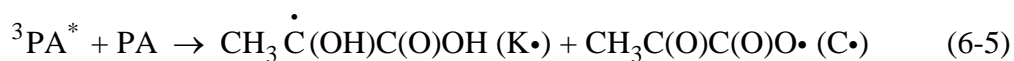
$$\log \phi_{\text{CO}_2} = (0.81 \pm 0.33) - (338 \pm 81)/T \quad (6-4)$$

in frozen PA solutions. Equation 6-4 leads to an extrapolated value of $\phi_{\text{CO}_2} = 0.45$ at 293 K, i.e., only ~ 40% smaller than in water ($\phi_{\text{CO}_2} = 0.78$).

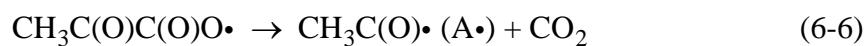
Mechanism of Reaction

The similar ϕ_{CO_2} values measured above and below the freezing point, and the fact that the organic products detected after thawing photolyzed frozen aqueous PA solutions are identical to those previously reported for the photolysis of fluid solutions, i.e., 2,3-

dimethyl tartaric (X), and 2-(3-oxobutan-2-yloxy)-2-hydroxypropanoic acids (Y),⁴² indicate that PA photolysis follows the same course in fluid and frozen solutions. The initial chemical transformation resulting from photon absorption likely involves an H-atom transfer between the excited $^3\text{PA}^*$ and a vicinal PA molecule:



The ketyl radical $\text{K}\cdot$ is rather stable and can engage in further reactions, but the decarboxylation of the acetylcarbonyloxyl radical $\text{C}\cdot$



takes place within a few vibrational periods, even at low temperatures.^{54,55} The observation that $\text{CO}_2(\text{g})$ is promptly released in the photolysis of frozen PA solutions down to at least $\sim 130 \text{ K}$ ⁴¹ is therefore consistent with a primary photochemical process, reaction 6-5, followed by a barrierless decomposition, reaction 6-6. Considering that all paramagnetic species, including free monoradicals, disappear irreversibly from previously irradiated frozen aqueous PA solutions above $\sim 190 \text{ K}$,⁴¹ $\text{A}\cdot$ and $\text{K}\cdot$ radicals subsequently undergo further reactions within nominally frozen matrices (see Scheme 1 in Ref. 42): $\text{K}\cdot + \text{PA} \rightarrow \text{C}\cdot$; $\text{C}\cdot + \text{A}\cdot \rightarrow \text{D}$; $\text{D} \rightarrow \text{Y} + \text{CO}_2$, which ultimately produce D (a C_8 β -oxocarboxylic acid), the immediate precursor of protracted CO_2 emissions. Notice that these bimolecular events must take place in quasi-fluid domains that allow the requisite molecular rotations and translations. These domains appear to support bimolecular reactions among radical species generated in close proximity, but prevent, however, radical scavenging by TEMPO at concentrations that had been effective in bulk aqueous solutions (see above).

The apparent Arrhenius parameters: $E_{a,D} = 22.8 \text{ kJ mol}^{-1}$, $A_D = 12.1 \text{ s}^{-1}$, associated with k_D , the pseudo-first-order rate constant for the decomposition of D in ice, are considerably smaller than those typical of the thermal decarboxylation of β -oxocarboxylic acids in aqueous solution ($E \sim 95 \text{ kJ mol}^{-1}$, A-factor $\sim 10^{12} - 10^{13} \text{ s}^{-1}$).⁵⁶ However, as pointed out above, they must still be associated with a chemical reaction (the thermal decarboxylation of D) rather than with physical desorption of preformed CO_2 . Stepped reaction kinetics in solids upon incremental warm-ups, such as the production and release of limited amounts of $\text{CO}_2(\text{g})$ from photolyzed samples after discrete temperature jumps (Figure 6-4), are typical of intrinsically fast reactions impeded by a cryogenic matrix.^{57,58}

Since the decarboxylation of β -ketoacids is an inherently difficult reaction involving four (or more) internal coordinates,^{56,59} it is conceivable that a rigid ice matrix could block its decomposition. Notice that: (1) $A_D = 12.1 \text{ s}^{-1}$ represents an impossibly large negative activation entropy for an elementary reaction: $\Delta S^\ddagger \sim -230 \text{ J K}^{-1} \text{ mol}^{-1}$,^{58,60} and (2) that $E_{a,D} = 22.8 \text{ kJ mol}^{-1}$ is nearly identical to the strength of the hydrogen bond in ice ($\sim 21 \text{ kJ mol}^{-1}$).^{61,62} Further confirmation that the decomposition of D is controlled by the ice matrix is provided by the fact that its estimated half-life, $\tau = 0.69/k_D > 10 \text{ min}$, in water at 293 K, as extrapolated from equation (6-3), would have given rise to slow CO_2 emissions from thawed irradiated samples, at variance with observations.

Photochemical Origin of CO and CO_2 Ice Core Records Irregularities

It is generally assumed that (given the prevalent low temperatures⁶³ and the fact that sunlight is completely blocked within a few meters below the surface by the highly

reflective snow/firn cover)⁶⁴⁻⁶⁷ species immobilized in deep ice core layers, i.e., below the firn line, will indefinitely retain their chemical identity. Thus, the fact that CO and CO₂ levels in Greenland ice core records dating from the last two millennia exceed those in contemporaneous Antarctic records by up to 130 ppbv and 20 ppmv (i.e., well beyond their experimental uncertainties), respectively,^{11,14} is an unexpected finding that seems to undermine the archival value of polar records and demands a plausible explanation. The anomalies are not restricted to interhemispheric differences, because CO₂ concentrations in Siple Dome, Antarctica, from certain periods of the Holocene are also larger than in other Antarctic sites by up to 20 ppmv.¹² The fact that outliers appear as sharp spikes superimposed on otherwise normal time series rules out analytical errors and militates against diffusional processes within the ice matrix. At stake is the issue of whether these anomalies are exceptional and, if so, why.

Several hypothesis have been advanced to account for the abnormal records.⁶⁸ The sudden occurrence of high CO concentrations at about 155 m depths suggests the presence of organic species that are able to produce carbon monoxide.¹⁴ The most probable explanation for CO₂ peak values in thin core sections representing only a few annual layers, or even less than an annual layer, specially in Greenland ice, is production of CO₂ by chemical reactions between impurities in the cold ice.¹¹ Possible CO₂ production mechanisms include:¹² (1) acidification of carbonates,^{13,16,69} (2) chemical,¹¹ or (3) biological oxidation of organic compounds.⁷⁰⁻⁷²

Both polar ice caps are known to be contaminated by organic material of continental or marine origin,⁷³⁻⁷⁵ but Greenland ice cores are conspicuously contaminated by snow scavenging of organic gases and deposition of the organic aerosol released by major,

sporadic, boreal forest fires.^{22,23,73,76} Full speciation of the organic matter present in polar ice remains a daunting analytical challenge,³³ but it is agreed that organic contaminants largely consist of humic-like substances, such as those globally present in natural waters, the simpler products of their solar photodegradation,^{24,28-30,77} as well as the products of organic aerosol photooxidation, such as dicarboxylic, α - and ω -oxocarboxylic acids, and α -dicarbonyl species.^{22,36,78,79} Pyruvic acid, 2-oxopropanoic acid, is a ubiquitous representative of these species.

The likelihood of the acid-carbonate reaction as the source of CO₂ spikes can be tested by comparing CO₂ and carbonate profiles in the ice cores, as proposed by Anklin et al.¹³ Such a test has now been performed at Dome Fuji, East Antarctica, where CO₂ was found to be uncorrelated with either Ca²⁺, a proxy for carbonate, or acidity.³⁷ Kawamura et al. estimate, from their measurements, that only 2–4% of the 10–20 ppmv excess CO₂ detected in 17–22 kyr old sections, could have originated from the *in situ* acidification of carbonate.³⁷ On the other hand, the uncatalyzed oxidation of organic matter by H₂O₂ is only viable for specific functionalities and is a slow reaction at best ($E_a = 36 \text{ kJ mol}^{-1}$ for the oxidation of formaldehyde).⁸⁰ The detection of unreacted hydrogen peroxide^{81,82} and organic matter in close proximity within ice cores after thousands of years supports the view that, unless specific catalysts were also present at the same location, this pathway is unlikely to produce carbon oxides from organic matter. The fact that most ice core sections are acidic and contain carbonates, organic material and oxidizing agents after thousands of years further suggests that mere reagent availability does not necessarily result in chemical reaction within glacial ice.⁸² The large activation energy ($E_a \sim 110 \text{ kJ mol}^{-1}$)⁷² associated with the metabolic activity of psychrophilic microbes should drastically

limit production rates of catabolic gases (such as CO₂ and CH₄) in the relatively shallow anomalous ice core sections (T < -40 °C down to ~ 1000 m depths).⁶³

The photochemical degradation of dissolved organic matter in the atmosphere, surface waters, and snow^{34,83} yields CO,^{27,30,84} and CO₂.²⁵ Quantum yields of CO₂ and CO photoproduction, which depend somewhat on the origin of dissolved organic matter, decrease exponentially at longer wavelengths.^{25,30} Relative yields vary in the range $20 \leq \phi_{\text{CO}_2} / \phi_{\text{CO}} \leq 50$. The possibility that photochemical processes similar to those occurring in surface waters could occur in deep ice, and therefore contaminate paleorecords, has been implicitly discounted due to the high reflectivity of the snow cover to ultraviolet light, the lack of a conceivable *in situ* source of actinic radiation, and the absence of documented examples of photoinduced decarboxylations/decarbonylations in frozen aqueous media. Still, “even the highly improbable must be considered over the long timescales involved in ice core chemistry. Organic acids and other C-containing species present in sufficient quantities have the potential to influence CO and CO₂, if a reasonable mechanism were proposed.”⁸⁵

We have recently proposed and quantified the likelihood that the dissolved organic matter trapped in ice cores could be photodegraded by the ultraviolet Cerenkov radiation generated by cosmic muons.³⁸ The timing and magnitude of the CO anomalies in Greenland vs. coeval Antarctic ice core bubbles dating from the Middle Ages could be plausibly correlated with the occurrence of boreal fires.²³ This analysis revealed that significant photochemistry could be induced in deep ice by Cerenkov radiation over geological periods. Despite the small local photon production rates, the exceptional transparency of pristine glacial ice between 200 and 500 nm^{86,87} allows chromophoric

point impurities, such as those created by sporadic contamination from dissolved organic matter, to be photochemically processed not only by locally generated photons, but also from those created elsewhere and collected onto the absorbing layer after diffusing through the ice matrix. A strongly absorbing sink effectively acts as an antenna whose collection efficiency is proportional to the ratio of the thickness of the pristine layer to the effective thickness of the layer containing the organic chromophore. This ratio depends, in general, on dust levels in the ice, as well as on chromophore concentration and absorptivity.³⁸

A photochemical mechanism provides a unified mechanism that largely accounts for both CO and CO₂ anomalies. Figure 6-7 compares CO¹⁴ and CO₂ excesses¹³ in Eurocore vs. the constant value (89 ppbv) for the period 1640–1870 AD, and Antarctic profiles as function of gas age, respectively. Not only are the trends similar, but the ratio of the slopes, $S_{\text{CO}_2}/S_{\text{CO}} \sim 200$, falls in the range of the ratio of quantum yields, $\phi_{\text{CO}_2}/\phi_{\text{CO}}$, for the production of dissolved inorganic carbon (that should appear as CO₂ in ice) and CO in the solar photolysis of dissolved organic matter in natural waters.²⁴⁻³¹ A more stringent comparison should, of course, involve ϕ 's for the photolysis of dissolved organic matter in ice by Cerenkov radiation in the range $200 < \lambda < 400$ nm, rather than in water under solar ($\lambda > 300$ nm) radiation. The data in Figure 6-7 are interpreted, therefore, as evidence that *in situ* photochemistry involving organic contaminants is the major, if not the exclusive, mechanism underlying ice core record anomalies.

Acknowledgment: This work was financed by NSF grant ATM-0228140. Nathan Dalleska (Caltech Environmental Analysis Center) provided valuable technical assistance.

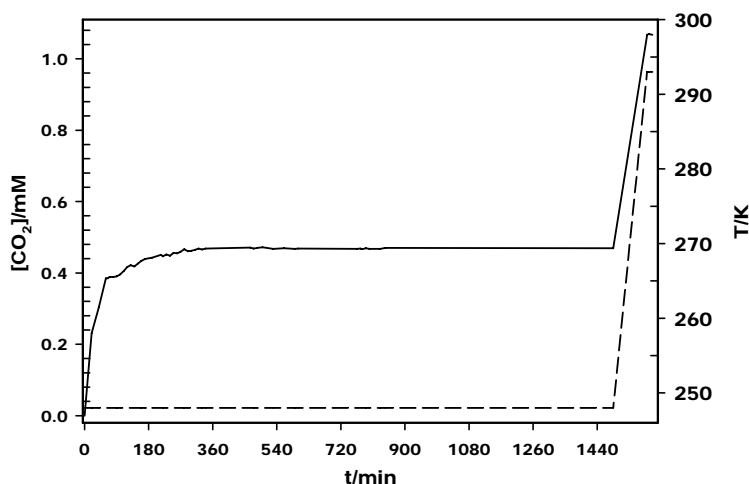


Figure 6-1. Solid trace (left axis): $\text{CO}_2(\text{g})$ released in the $\lambda \sim 313$ nm photolysis of frozen, deaerated aqueous pyruvic acid (4 mL, 100 mM, pH 1.0) solutions. $\text{CO}_2(\text{g})$ is released during the initial 60 min irradiation period, and also in the post-illumination stage. Additional $\text{CO}_2(\text{g})$ is liberated upon thawing. Dashed trace (right axis): sample temperature.

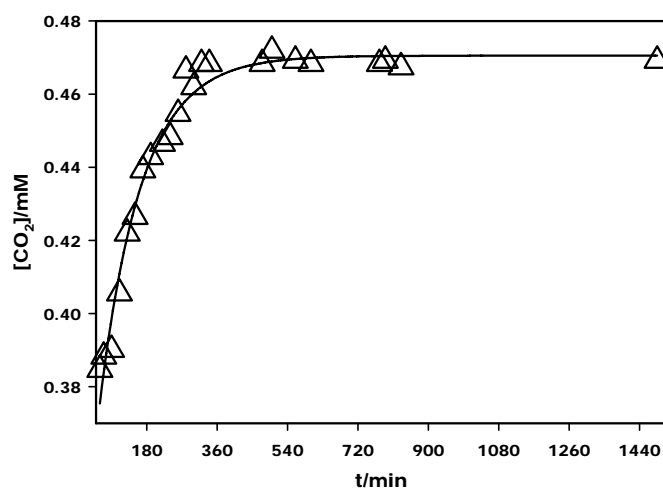


Figure 6-2. (Δ) Blow up of post-irradiation $\text{CO}_2(\text{g})$ data from the experiment of Figure 6-1. Solid trace: $[\text{CO}_2] = A + B [1 - \exp(-k_D \times \text{time})]$; $A = 0.304$ mM; $B = 0.167$ mM; $k_D = 9.307 \times 10^{-3} \text{ min}^{-1}$.

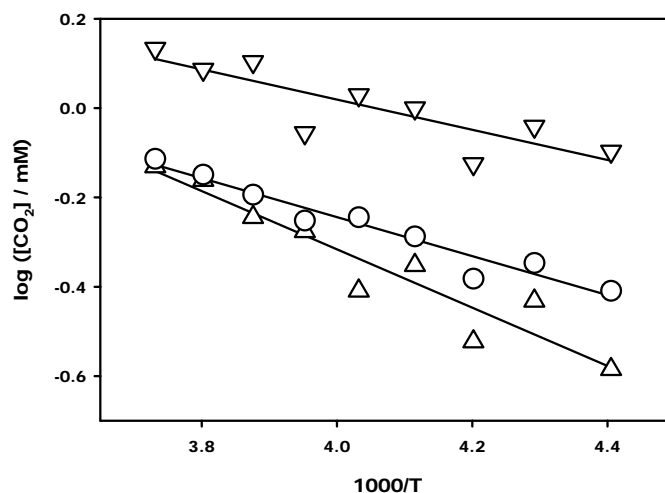


Figure 6-3. $\text{CO}_2(\text{g})$ released in the isothermal photolysis of frozen, deaerated aqueous pyruvic acid (4 mL, 100 mM, pH 1.0) solutions as function of temperature.

(Δ) immediately after photolysis; (\circ) before sample thawing; (∇) after sample thawing.

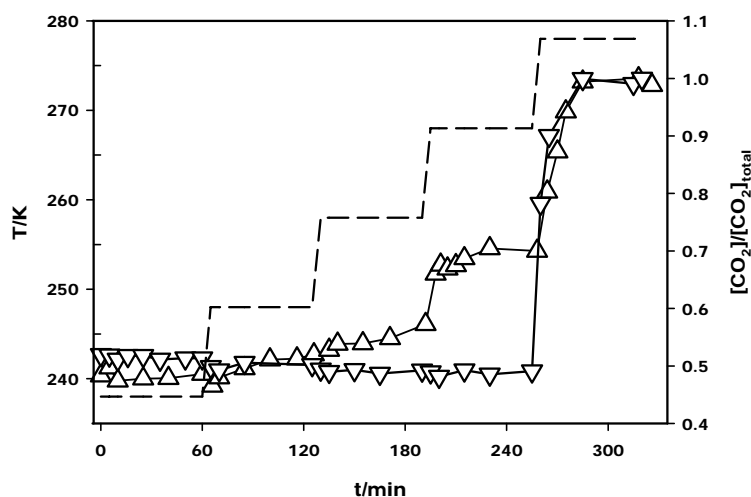


Figure 6-4. Symbols and solid traces (right axis): normalized $\text{CO}_2(\text{g})$ amounts released in post-irradiation periods. (Δ) after 60 min photolysis of frozen, deaerated aqueous pyruvic acid (4 mL, 100 mM, pH 1.0). (∇) after 15 min photolysis of frozen, deaerated aqueous benzoylformic acid (4 mL, 10 mM, pH 1.0). Dashed trace (left axis): sample temperature.

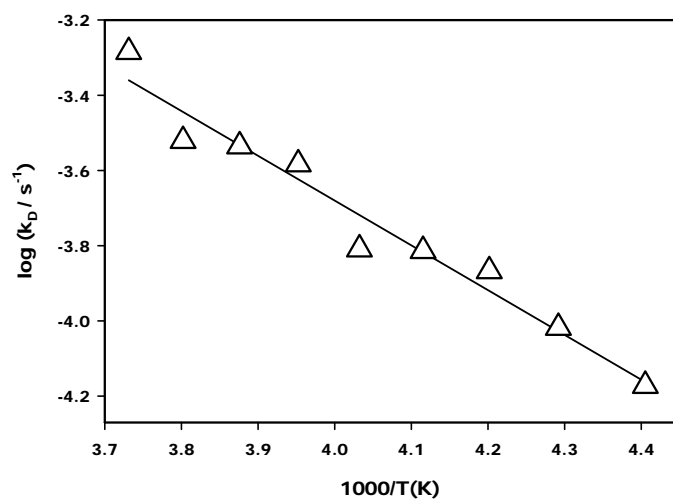


Figure 6-5. (Δ) Experimental first-order rate constants k_D (T) for the release of $\text{CO}_2(\text{g})$ from previously photolyzed frozen pyruvic acid solutions. Solid trace: $\log(k_D/\text{s}^{-1}) = 1.08 - 1191/T$.

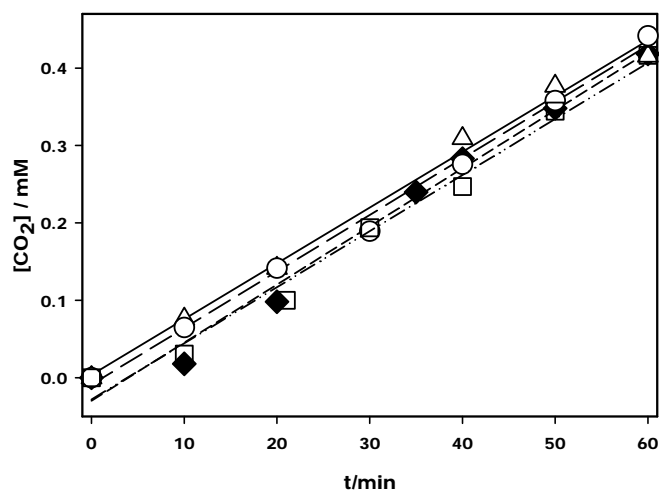


Figure 6-6. $\text{CO}_2(\text{g})$ released during irradiation of frozen, deaerated aqueous pyruvic acid (4 mL, 100 mM, pH 1.0) doped with TEMPO at 253 K. (Δ) without TEMPO; (\blacklozenge) $[\text{TEMPO}] = 0.253$ mM; (\circ) $[\text{TEMPO}] = 0.994$ mM; (\square) $[\text{TEMPO}] = 2.403$ mM.

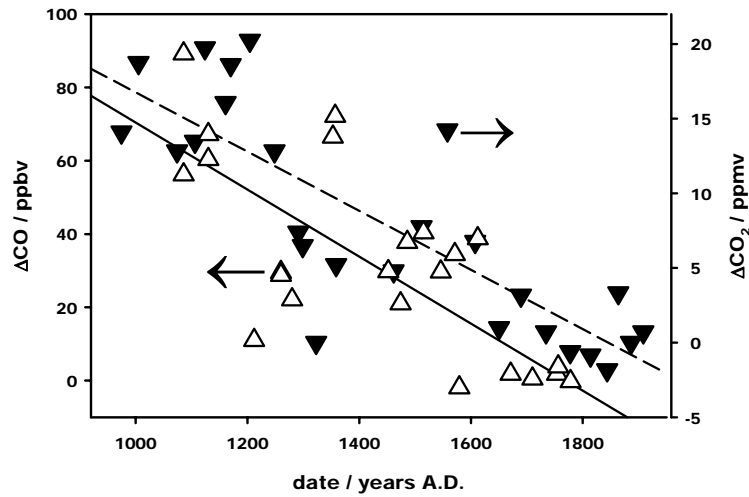


Figure 6-7. (▼) Differences between CO₂ (ppmv, right axis) readings from Greenland (Eurocore, GRIP) and Antarctic (South Pole: D47, D57) ice core records versus date.¹³
 (△) Differences between CO (ppbv, left axis) readings from Greenland (Eurocore, GRIP) relative to the constant value (89 ppbv) for the period 1640–1870 AD versus date.¹⁴

References

- 1- Wolff, E. W. *Antarctic Sci.* **2005**, *17*, 487.
- 2- Brook, E. J. *Science* **2005**, *310*, 1285.
- 3- EPICA. *Nature* **2004**, *429*, 623.
- 4- North Greenland Ice Core Project Members. *Nature* **2004**, *431*, 147.
- 5- Fischer, H.; Wahlen, M.; Smith, J.; Mastroianni, D.; Deck, B. L. *Science* **1999**, *283*, 1712.
- 6- Stauffer, B. *Space Sci. Rev.* **2000**, *94*, 321.
- 7- Landais, A.; Barnola, J. M.; Kawamura, K.; Caillon, N.; Delmotte, M.; Van Ommen, T.; Dreyfus, G.; Jouzel, J.; Masson-Delmotte, V.; Minster, B.; Freitag, J.; Leuenberger, M.; Schwander, J.; Huber, C.; Etheridge, D.; Morgan, V. *Quaternary Sci. Rev.* **2006**, *25*, 49.
- 8- Boucot, A. J.; Gray, J. *Earth Sci. Rev.* **2001**, *56*, 1.
- 9- Mudelsee, M. *Quaternary Sci. Rev.* **2001**, *20*, 583.
- 10- Pearson, P. N.; Palmer, M. R. *Nature* **2000**, *406*, 695.
- 11- Tschumi, J.; Stauffer, B. *J. Glaciol.* **2000**, *46*, 45.
- 12- Ahn, J.; Wahlen, M.; Deck, B. L.; Brook, E. J.; Mayewski, P. A.; Taylor, K. C.; White, J. W. C. *J. Geophys. Res.* **2004**, *109*, D13305.
- 13- Anklin, M.; Barnola, J. M.; Schwander, J.; Stauffer, B.; Raynaud, D. *Tellus B* **1995**, *47*, 461.
- 14- Haan, D.; Raynaud, D. *Tellus* **1998**, *50 B*, 253.
- 15- Stauffer, B.; Fluckiger, J.; Monnin, E.; Schwander, M.; Barnola, J. M.; Chappellaz, J. *Ann. Glaciol.* **2002**, *35*, 202.

- 16- Delmas, R. J. *Tellus* **1993**, 45B, 391.
- 17- Stauffer, B.; Blunier, T.; Dallenbach, A.; Indermuhle, A.; Schwander, J.; Stocker, T. F.; Tschumi, J.; Chappellaz, J.; Raynaud, D.; Hammer, C. U.; Clausen, H. B. *Nature* **1998**, 392, 59.
- 18- Haan, D.; Martinerie, P.; Raynaud, D. *Geophys. Res. Lett.* **1996**, 23, 2235.
- 19- Andres, E.; et, a. *Nature* **2001**, 410, 441.
- 20- Cowen, D. F.; Andres, E.; Askebjerg, P. et al., *Internat. J. Mod. Phys. A* **2001**, 16, 1013.
- 21- Burden, D. L.; Hieftje, G. M. *Anal. Chem.* **1998**, 70, 3426.
- 22- Kawamura, K.; Yokoyama, K.; Fujii, Y.; Watanabe, O. *J. Geophys. Res.* **2001**, 106, 1331.
- 23- Savarino, J.; Legrand, M. *J. Geophys. Res.* **1998**, 103, 8267.
- 24- Gao, H. Z.; Zepp, R. G. *Environ. Sci. Technol.* **1998**, 32, 2940.
- 25- Johannessen, S. C.; Miller, W. L. *Marine Chemistry* **2001**, 76, 271.
- 26- Kieber, D. J.; McDaniel, J.; Mopper, K. *Nature* **1989**, 341, 637.
- 27- Mopper, K.; Zhou, X.; Kieber, R. J.; Sikorski, R. G.; Jones, R. D. *Nature* **1991**, 353, 60.
- 28- Moran, M. A.; Zepp, R. G. *Limnol. Oceanogr.* **1997**, 42, 1307.
- 29- Opsahl, S. P.; Zepp, R. G. *Geophys. Res. Lett.* **2001**, 28, 2417.
- 30- Valentine, E. L.; Zepp, R. G. *Environ. Sci. Technol.* **1993**, 27, 409.
- 31- Zuo, Y.; Jones, R. D. *Geophys. Res. Lett.* **1996**, 23, 2769.
- 32- Calace, N.; Petronio, B. M.; Cini, R.; Stortini, A. M.; Pampaloni, B.; Udisti, R. *Internat. J. Environ. Anal. Chem.* **2001**, 79, 331.

- 33- Grannas, A. M.; Hockaday, W. C.; Hatcher, P. G.; Thompson, L. G.; Mosley-Thompson, E. *J. Geophys. Res.* **2006**, *111*, D04304.
- 34- Grannas, A. M.; Shepson, P. B.; Filley, T. R. *Global Biogeochem. Cycles* **2004**, *18*, GB1006.
- 35- Grannas, A. M.; Shepson, P. B.; Guimbaud, C.; Sumner, A. L.; Albert, M.; Simpson, W.; Domine, F.; Boudries, H.; Bottenheim, J.; Beine, H. J.; Honrath, R. E.; Zhou, X. L. *Atmos. Environ.* **2002**, *36*, 2733.
- 36- Kawamura, K.; Imai, Y.; Barrie, L. A. *Atmos. Environ.* **2005**, *39*, 599.
- 37- Kawamura, K.; Nakazawa, T.; Aoki, S.; Sugawara, S.; Fujii, Y.; Watanabe, O. *Tellus* **2003**, *55 B*, 126.
- 38- Colussi, A. J.; Hoffmann, M. R. *Geophys. Res. Lett.* **2003**, *30*, 1195.
- 39- Budac, D.; Wan, P. *J. Photochem. Photobiolog. A: Chem.* **1992**, *67*, 135.
- 40- Wan, P.; Budac, D. *CRC Handbook of Organic Photochemistry and Photobiology*; CRC Press: Boca Raton, 1995.
- 41- Guzmán, M. I.; Colussi, A. J.; Hoffmann, M. R. *J. Phys. Chem. A* **2006**, *110*, 931.
- 42- Guzmán, M. I.; Colussi, A. J.; Hoffmann, M. R. *J. Phys. Chem. A* **2006**, *110*, 3619.
- 43- Gorner, H.; Khun, H. J. *J. Chem. Soc., Perkin Trans., 2* **1999**, 2671.
- 44- Beckwith, A. L. J.; Bowry, V. W.; Ingold, K. U. *J. Am. Chem. Soc.* **1992**, *114*, 4983.
- 45- Bowry, V. W.; Ingold, K. U. *J. Am. Chem. Soc.* **1992**, *114*, 4992.
- 46- Fischer, H. *Chem. Rev.* **2001**, *101*, 3581.
- 47- Buschmann, H. J.; Dutkiewicz, E.; Knoche, W. *Ber. Bunsenges. Phys. Chem.* **1982**, *86*, 129.

- 48- Buschmann, H. J.; Fuldner, H. H.; Knoche, W. *Ber. Bunsenges. Phys. Chem.* **1980**, *84*, 41.
- 49- Guzmán, M. I.; Hildebrandt, L.; Colussi, A. J.; Hoffmann, M. R. *J. Am. Chem. Soc.* **2006**, *128*, 10621.
- 50- Fleury, M. B.; Moiroux, J.; Fleury, D.; Dufresne, J. C. *J. Electroanal. Chem.* **1977**, *81*, 365.
- 51- Kuhn, H. J.; Gorner, H. *J. Phys. Chem.* **1988**, *92*, 6208.
- 52- Dubowski, Y.; Colussi, A. J.; Hoffmann, M. R. *J. Phys. Chem. A* **2001**, *105*, 4928.
- 53- Leermakers, P. A.; Vesley, G. F. *J. Am. Chem. Soc.* **1963**, *85*, 3776.
- 54- Abel, B.; Assmann, J.; Buback, M.; Grimm, C.; Kling, M.; Schmatz, S.; Schroeder, J.; Witte, T. *J. Phys. Chem. A* **2003**, *107*, 9499.
- 55- Bockman, T. M.; Hubig, S. M.; Kochi, J. K. *J. Org. Chem.* **1997**, *62*, 2210.
- 56- Guthrie, J. P. *Bioorg. Chem.* **2002**, *30*, 32.
- 57- Spath, B. W.; Raff, L. M. *J. Phys. Chem.* **1992**, *96*, 2179.
- 58- Andraos, J. *J. Phys. Chem. A* **2000**, *104*, 1532.
- 59- Huang, C. L.; Wu, C. C.; Lien, M. H. *J. Phys. Chem. A* **1997**, *101*, 7867.
- 60- Benson, S. W. *Thermochemical Kinetics*, 2nd ed.; Wiley: New York, 1976.
- 61- Cotton, F. A.; Wilkinson, G. *Advanced Inorganic Chemistry*, 4th ed.; Wiley: New York, 1980.
- 62- Galwey, A. K.; Sheen, D. B.; Sherwood, J. N. *Thermochim. Acta* **2001**, *375*, 161.
- 63- Price, P. B.; Nagornov, O. V.; Bay, R.; Chirkin, D.; He, Y. D.; Miocinovic, P.; Richards, A.; Woschnagg, K.; Koci, B.; Zagorodnov, V. *Proc. Natl. Acad. Sci. U. S. A.* **2002**, *99*, 7844.

- 64- Belzile, C.; Johannessen, S. C.; Gosselin, M.; Demers, S.; Miller, W. L. *Limn. and Oceanogr.* **2000**, *45*, 1265.
- 65- Gerland, S.; Winther, J. G.; Orbaek, J. B.; Liston, G. E.; Oritsland, N. A.; Blanco, A.; Ivanov, B. *Hydrological Processes* **1999**, *13*, 2331.
- 66- Glendinning, J. H. G.; Morris, E. M. *Hydrological Processes* **1999**, *13*, 1761.
- 67- Phillips, G. J.; Simpson, W. R. *J. Geophys. Res.* **2005**, *110*, D08306.
- 68- Monnin, E.; Indermuhle, A.; Dallenbach, A.; Fluckiger, J.; Stauffer, B.; Stocker, T. F.; Raynaud, D.; Barnola, J. M. *Science* **2001**, *291*, 112.
- 69- Barnola, J. M.; Anklin, M.; Porcheron, J.; Raynaud, D.; Schwander, J.; Stauffer, B. *Tellus* **1995**, *47 B*, 264.
- 70- Campen, R. K.; Sowers, T.; Alley, R. B. *Geology* **2003**, *31*, 231.
- 71- Mader, H. M.; M.E., P.; Wadham, J. L.; Wolff, E. W.; Parkes, R. J. *Geology* **2006**, *34*, 169.
- 72- Price, P. B.; Sowers, T. *Proc. Natl. Acad. Sci. USA* **2004**, *101*, 4631.
- 73- Kawamura, K.; Kasukabe, H.; Yasui, O.; Barrie, L. A. *Geophys. Res. Lett.* **1995**, *22*, 1253.
- 74- Gayley, R. I.; Ram, M. *J. Geophys. Res.* **1985**, *90*, 12921.
- 75- Desideri, P. G.; Lepri, L.; Udisti, R.; Checchini, L.; Del Bubba, M.; Cini, R.; Stortini, A. M. *Internat. J. Environ. Anal. Chem.* **1998**, *71*, 331.
- 76- Domine, F.; Shepson, P. B. *Science* **2002**, *297*, 1506.
- 77- Miller, W. M.; Zepp, R. G. *Geophys. Res. Lett.* **1995**, *22*, 417.
- 78- Wang, H.; Kawamura, K.; Yamazaki, K. *J. Atmos. Chem.* **2006**, *53*, 43.
- 79- Kawamura, K.; Kasukabe, H.; Barrie, L. A. *Atmos. Environ.* **1996**, *30*, 1709.

- 80- Do, J. S.; Chen, C. P. *J. Appl. Electrochem.* **1994**, *24*, 936.
- 81- Hutterli, M. A.; McConnell, J. R.; Bales, R. C.; Stewart, R. W. *J. Geophys. Res.* **2003**, *108*, D4023.
- 82- Sigg, A.; Neftel, A. *Nature* **1991**, *351*, 557.
- 83- Osburn, C. L.; Morris, D. P.; Thorn, K. A.; Moeller, R. E. *Biogeochemistry* **2001**, *54*, 251.
- 84- Schade, G. W.; Hofmann, R. M.; Crutzen, P. J. *Tellus* **1999**, *51 B*, 889.
- 85- Wolff, E. W. *NATO ASI Series I* **1996**, *43*, 541.
- 86- Askebjør, P.; Barwick, S. W.; Bergstrom, L.; et al. *Geophys. Res. Lett.* **1997**, *24*, 1355.
- 87- Askebjør, P.; Barwick, S. W.; Bergstrom, et al. *Appl. Optics* **1997**, *36*, 4168.